Available online at www.sciencedirect.com
ScienceDirect
Dyes and Pigments 73 (2007) 298–304
DYES and PIGMENTS
www.elsevier.com/locate/dyepig

Variables affecting the antibacterial properties of nano and pigmentary titania particles in suspension

J. Verran [a,*], G. Sandoval [a], N.S. Allen [a], M. Edge [a], J. Stratton [b]

[a] *Department of Biology, Chemistry and Health Science, Dalton Research Institute, Manchester Metropolitan University, John Dalton Building, Chester Street, Manchester M1 5GD, UK*
[b] *Millenium Inorganic Chemicals, PO Box 26, Grimsby, NE Lincs, DN41 8DP, UK*

Received 3 October 2005; accepted 6 January 2006
Available online 7 March 2006

Abstract

The antibacterial activity of photoactivated nano and pigmentary titania particles in suspension was evaluated using *Escherichia coli* as the target organism. The antibacterial activity of nanotitanium particles was determined more by their intrinsic ability to generate radicals than to particle size. Indeed there was an inverse relationship between particle size and activity. The antibacterial activity of the particles was affected by multiple experimental parameters. The reliability and variability of the results were affected by the physiological status of the bacterial cells, the initial cell concentration, and the set up of the irradiation system and were also improved if the cell–particle mixture was stirred during irradiation. The development of appropriate in vitro testing methods is essential in the determination of antimicrobial effectiveness of these particles and this is examined here coupled with the use of the microwave spectroscopic method for determining the photoactivity of the pigments in terms of carrier generation.
© 2006 Elsevier Ltd. All rights reserved.

Keywords: Photocatalytic; Antibacterial; Titanium dioxide; Pigments; Nanoparticles; *Escherichia coli*

1. Introduction

When light energy of wavelength below 400 nm is utilised by the photocatalytic action of titanium dioxide, the free radicals produced can decompose or destroy foreign materials. An antibacterial effect has been demonstrated, with several groups describing antimicrobial effects of suspensions of particles, or thin films [1–6]. Most of this work has been carried out using the anatase pigment P25 (Degussa Chemical Company, Germany).

The thermal and photocatalytic activity of a selection of nano versus micron-sized anatase and rutile titania pigments in polyethylene and alkyd based paint films has already been assessed in our laboratories [7–10]. Preliminary experiments demonstrated an antibacterial effect of the pigments by irradiation of a mixture of bacterial cell suspensions and pigment mixtures [9–11]. Further work was carried out to clarify the relative activities of the pigment series in terms of antibacterial effects, and to define experimental variables which may affect a demonstrable in vitro antibacterial activity. We believe that this is the first study using a range of nanoparticle TiO_2 pigments with different particle sizes for monitoring the inactivation/destruction of bacteria. Coupled within this study is the use of the photodielectric microwave method for analysis and comparing the titania activities for cross-referencing [12,13].

2. Experimental

2.1. Materials

A range of anatase and rutile pigments (supplied by Millenium Inorganic Chemicals, Grimsby, UK) were used in the

* Corresponding author. Tel.: +44 161 247 1206; fax: +44 161 247 6325.
E-mail address: j.verran@mmu.ac.uk (J. Verran).

0143-7208/$ - see front matter © 2006 Elsevier Ltd. All rights reserved.
doi:10.1016/j.dyepig.2006.01.003

study (Table 1). The most active photocatalysts are formulations based on the anatase crystal phase, and most work [15,16] has been carried out on pigment B (Degussa P25). In contrast to the remaining pigments, which were supplied as powders, pigment C is a colloidal dispersion of nanoparticles (colloidal suspension of TiO_2, 14–16%, stabilised with an amine, with a pH of 10–11.5). This suspension was neutralised with HCl to remove the amine, and to reduce the pH, and was then washed with water to remove the salt. It consisted of 1–10 nm primary particles, as determined by XRD, with 45–50 nm agglomerate size as indicated by transmission electron microscopy. This colloidal dispersion is the precursor product from which the rest of the pigments were produced, either by drying (pigment G), or calcining at increasing temperatures (pigments F, E, A). Pigments were characterised using microwave spectroscopy [7].

Stock suspensions were prepared by mixing 0.05 g TiO_2 in 5 ml deionised water. The dispersion was vortex mixed for 1 min, and was then diluted to 25 ml in order to produce a 0.2% stock suspension, from which required concentrations were prepared using deionised water.

2.2. Culture preparation

Escherichia coli NCTC 9001 was used as a model microorganism for all inactivation studies. In preparation for inactivation experiments, one colony from a 24 h culture on nutrient agar was inoculated into 10 ml nutrient broth and incubated at 37 °C for 24 h. Washed cell suspensions were prepared by centrifugation of cultures for 10 min at 3000 rpm. The supernatant was discarded and the pellet was re-suspended in deionised water, three times, with the final re-suspension in 10 ml deionised water, to prevent carryover of nutrient from the original culture medium [17], and hence any unintentional increase in cell numbers, or effect on cell physiology [19]. The optical density of the suspension at 460 nm was taken, and its value adjusted to approximately 0.91 by adding or removing (by centrifugation and re-suspension in a reduced volume) water as necessary. The concentration of the suspension was determined by diluting 1 ml of the sample 10-fold, plating 0.1 ml of each dilution onto nutrient agar in triplicate, and counting the resultant colonies. It is assumed that one cell (or one cluster of cells) will multiply on the medium to produce a visible colony.

The dilution at which the maximum number of countable colonies was obtained was used to calculate the number of viable cells per milliliter of original suspension. This was approximately 10^8 colony forming units (cfu) per ml. One milliliter of 10^6 cfu/ml was mixed with the required amount of TiO_2 stock suspension, and then diluted with deionised water to give a total volume of 25 ml with a final cell concentration of 10^5 cfu/ml.

2.3. Irradiation

After vortex mixing, the 25 ml cell–pigment mixture was poured into a 100 ml Petri dish on a magnetic cold plate and irradiated. Illumination was provided by a Hg–Zn–Cd (0.9 A) lamp (Philips) located 10 cm from the suspension. The suspension depth was approximately 5 mm. The mixture was mixed continuously using a sterilised Teflon coated magnetic stir bar placed in the Petri dish. Samples of 1 ml were removed at specific times during irradiation, and were diluted 10-fold, with 0.1 ml of each dilution being plated in triplicate onto nutrient agar for determination of survivors (expressed as cfu/ml).

It is important to maintain a septic technique when manipulating microorganisms, to prevent contamination. All materials were sterile. The irradiation experiments were performed at room temperature (25 °C), but during irradiation, the temperature within the suspension could rise to 32 °C.

2.4. Experimental variables

In order to devise the procedure outlined above, a number of experimental variables were monitored in the series of experiments:

(i) *Elimination of wavelengths with intrinsic antibacterial activity*: in later experiments, a Pyrex glass filter was placed over the Petri dish in order to eliminate wavelengths below and around 310 nm, since the Hg lamp emitted a high output below 300 nm, with intrinsic antimicrobial activity.

(ii) *Use of washed cell suspensions*: in later experiments, the cell suspension was not washed, but was mixed with titanium particles in the nutrient broth culture medium.

Table 1
Main properties of pigments used for antibacterial disinfection by TiO_2

Pigment	Crystalline modification	BET surface area (M^2/g)	Particle size	Preparation method	Dispersibility	Treatment
A	Micro-anatase	10.1	0.24 μm	Sulphate route	Medium	1% Alumina
B (Degussa P25)	Anatase-rutile	50	25–35 nm	Flame hydrolysis	Good	
C (colloid)	Nano-anatase	329.1	5–10 nm	Sulphate route	Good	
D	Micro-rutile	12.4	0.11 μm	Chloride route	Poor	3.4% Alumina
E	Nano-anatase	44.4	20–30 nm	Sulphate route	Poor	
F	Nano-anatase	77.9	15–25 nm	Sulphate route	Poor	
G	Nano-anatase	329.1	5–10 nm	Sulphate route	Poor	
H	Nano-anatase	52.1	70 nm	Sulphate route	Medium	Hydroxyapatite

(iii) *Standardisation of cell suspensions*: the effect on variability of using the same standardised washed cell suspension several times within one day was monitored. A reduction in the number of viable cells in the suspension was noted during an 8 h day, coupled with a slightly enhanced antibacterial effect of the nanoparticles observed across 4 repeat experiments carried out in series through one day. Thus the 24 h cell suspensions in culture medium were used, with the culture medium providing some protection to the cells compared with the stress placed on them by suspension in deionised water, which was clearly affecting viability and susceptibility to photoactivity. Since cells were in stationary phase [19], it was anticipated that an increase in cell numbers due to growth during the experiment was unlikely. As a result of this modification, the reproducibility was improved. In addition, standardisation of the optical density of the inoculum also proved beneficial in this context. Some degree of variability is, however, inevitable in microbiology.

(iv) *Sedimentation of pigments*: many of the pigments sedimented in suspension in the absence of stirring. In this situation, P25 was the most effective antibacterial pigment. The antibacterial effect of pigment C, a colloid dispersion, was comparable with P25 in unstirred conditions. These two pigments were dispersed preparations, thus with reduced sedimentation.

(vii) *Dispersion of pigments*: to determine the importance of dispersion and aggregation on antibacterial activity, pigment C was dried in an oven at 110 °C overnight, and was retested for antibacterial activity after grinding with a pestle and mortar.

Since the pigments with the best dispersion were the most effective, all other pigments were milled in order to produce particles of primary size and dispersibility, using high energy planetary milling and the dispersing agent Calgon. The dispersant agent was essential, since after planetary mixing in its absence, the particles reaggregated and antibacterial activity was not enhanced.

(viii) *Final experimental conditions*: once the key experimental factors had been defined, the powder pigment samples were screened using unwashed cells, stirred plates and a glass filter was placed over the Petri dish.

2.5. Microwave dielectric spectroscopy

The technique of microwave dielectric spectroscopy for measurement of titania photoactivity has been described in several articles [12,13]. Microwave measurements were undertaken using a Marconi (6200A) 2–20 GHz programmable sweep generator and automatic amplitude analyser, coupled to a circular waveguide and cylindrical cavity. Powdered samples (0.2 g) were packed in the bottom of the cavity on a plastic dish (to ensure reproducibility) and were irradiated in the cell chamber with an ILC 302UV xenon source via an optical fibre set up (Laser Lines Ltd., Beaumont Close, Banbury, Oxon, UK) switchable between UV and visible light with a cut-off point at 400 nm. In this work visible light only was used as the UV response is weak for the titania pigments. Changes in microwave cavity resonant frequency and attenuation of microwave power were monitored during 1800 s of irradiation and for 1800 s after switching off the light source (unless stated otherwise). All measurements were carried out in triplicate, and at 25 °C. The uncertainty in the values of 'shift in microwave cavity resonant frequency' is of the order ± 0.0004 GHz; while that for 'attenuated power' is ±0.05 dBm.

3. Results and discussion

3.1. Microwave analysis

In this technique microwaves are directed, via a waveguide, through an aperture into a cavity. At certain frequencies the cavity abstracts appreciable power, since the oscillating electric and magnetic fields of the microwave energy reach a maximum when they are resonant with the cavity. Typical microwave spectra for a selection of the anatase and rutile pigments used here with respect to that for the cavity have been illustrated earlier [12,13]. The amount of energy stored by a microwave cavity is known as its quality factor (*Q*-factor). When a sample is placed in the cavity and exposed to UV/vis light the position of the resonant frequency shifts and microwave power is attenuated.

The attenuation of microwave power is proportional to the changes in conductivity of the sample as free carriers are produced. This is due to the creation of large numbers of phonons (heat) by the free carriers, so reducing the ability of the microwave cavity to store energy. The magnitude of the resonant frequency shift is a measure of the extent to which the electric charge distribution in the sample can be distorted or polarized by the electric field. The nature and concentration of both free and trapped carriers in the sample will influence this effect.

Data from the microwave spectroscopy demonstrated the inherent photoactivity of the pigments used here (Fig. 1). The quality factor shift is positive and originates from free electrons promoted from the valence up to the conduction band. The data depicted relate to the response of the titanium dioxide powders in terms of changes of the microwave power

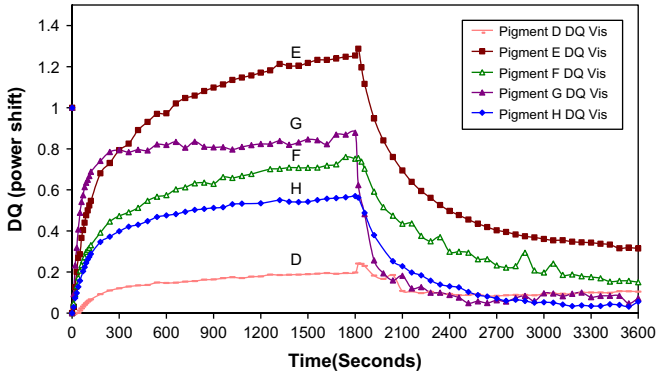

Fig. 1. Shift of cavity microwave power for titania pigments during consecutives periods of light exposure and darkness under UV light.

(DQ). The changes in the microwave power by the pigments are proportional to the changes in conductivity as free carriers are produced. Hence, higher values of DQ (shift of power) result from the generation of more active species by the pigment when exposed to light. During irradiation, the change in microwave power is lower in the case of alumina coated rutile pigment D. This is consistent with a reduction in free carrier population and enhanced trapping and recombination for the more heavily coated grade D.

The nanoparticles E, F and G all exhibit greater carrier generation than the rutile pigment D – hence greater activity. The hydroxyapatite coated pigment H also exhibits considerable free carrier generation under UV light illumination:

$$E > G > F > H$$

The rapid recombination rate of pigment G is obvious. This property will undoubtedly decrease its overall activity in a real system as their carriers recombine much faster. Table 2 depicts the free carriers' relaxation lifetime after switching of the light for comparison purposes by measuring the time it takes for the quality factor after 1800 s (Q_0) to decrease to Q_0/e.

It is evident from Table 2 that the relaxation times for the free carriers generated in pigment G are considerably lower than those in pigments E and F. These results prove that the crystallite structure is a main factor influencing photoactivity. Poor crystallinity and defects on crystal planes are responsible for the relative low life of the free carriers of pigment G in comparison with pigments F and E.

The nanoparticles E, F and G show an interesting behaviour. They all exhibit greater carrier generation than the rutile pigments hence greater activity. There are various factors that explain the higher activity of the nanoparticle products relative to pigmentary TiO_2. To begin with, blue shifts caused by nanoscale effects enhance the band gap, which in turn increases the redox potential. One of the major limitations in semiconductor photocatalysis is the relatively low value of the overall quantum efficiency mainly because of the high rate of recombination of photoinduced electron–hole pairs at or near the surface. Some success in enhancing the efficiencies of photocatalysts can been achieved using nano-sized semiconductor crystallites instead of bulk materials. Usually, electrons and holes need to diffuse to catalyst surfaces, where they are captured by electron and hole acceptors. If the dimensions of nanoscale particles are so small that the diffusion of electrons and holes to the surfaces is faster than the recombination process, the photoefficiency would be enhanced by employing such ultra-small particles. In comparison with bulk semiconductors, the nanoscale semiconductor retards the electron–hole recombination via charge carrier trapping. Hence, the separation efficiency of photoinduced carriers is very high for semiconductor nanoparticles, so that the activity of semiconductor nanoparticles may be higher than that of conventional semiconductor particle, that is to say, the smaller the size of semiconductor particle is, the higher the photocatalytic activity may be.

Table 2
Free carriers relaxation lifetimes (s) for nanoparticle pigments

Pigment	Relaxation time Visible light	Relaxation time UV light
E	1093	695
F	>1800	750
G	125	88
H	480	340

However, our experimental results are in contradiction with this speculation because crystalline structure is another factor influencing photoactivity. From our experimental results, there is an inverse correlation between activity and particle size where the nanoparticle with the highest particles size shows the highest activity and the nanoparticle with the highest surface area, pigment G shows the lowest production of free carriers (Fig. 2). This effect is explained by the improved crystallinity of the nanoparticle pigment calcined at the highest temperature. Pigments E and F present lower concentrations of defects compared with pigment G and therefore less recombination centres, hence greater carrier generation is shown by these two pigments. Pigment G, after a fast initial rise in carrier production, displays a strong plateau due to strong trapping followed by a sharp dark decay to the valence state after extinguishing the light source, due to carrier recombination. Pigment G, did not suffer any thermal treatment to improve its crystallinity, it was just dried. Hence, the lower crystallinity of this compound induces a high concentration of defects that are able to trap out the carriers. No such rapid dark recombinations were evident in the case of the pigments E and F. The dark recombination process in pigments E and F suggests that excess carriers are trapped in deep lying states giving rise to the observed long lived residual component in the decay process. A high level of crystallinity compensates the lower specific surface area of pigment E. This crystallinity results in a higher efficiency generating free carriers.

3.2. Antibacterial activity

Results for antibacterial activity correlated with the microwave data sequence. Overall, there was (Fig. 3) an inverse relationship between antibacterial activity and particle size: for the pigment powders, pigment $E > H > F > G = A$, with

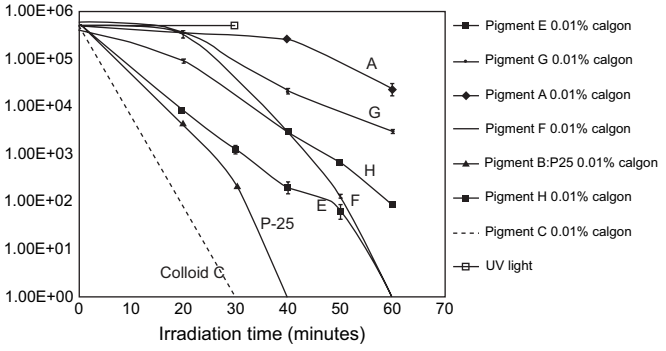

Fig. 2. Photocatalytic bactericidal effect of pigments A, B, E, F, G, H powders and C (colloid) at 0.01% in stirred conditions, unwashed cell suspensions.

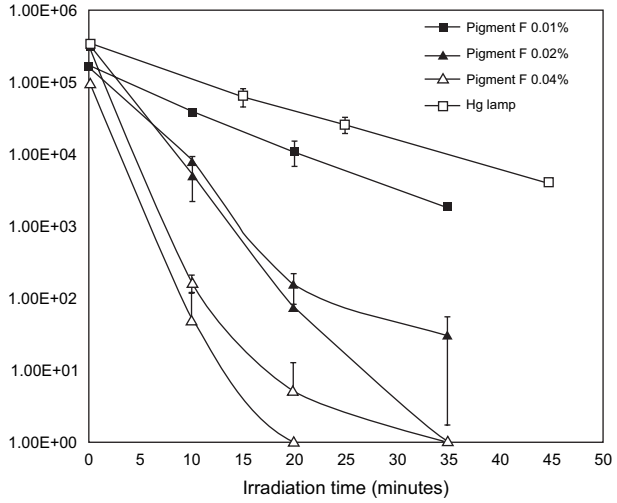

Fig. 3. Effect of concentration of pigment F on photocatalytic bactericidal effect.

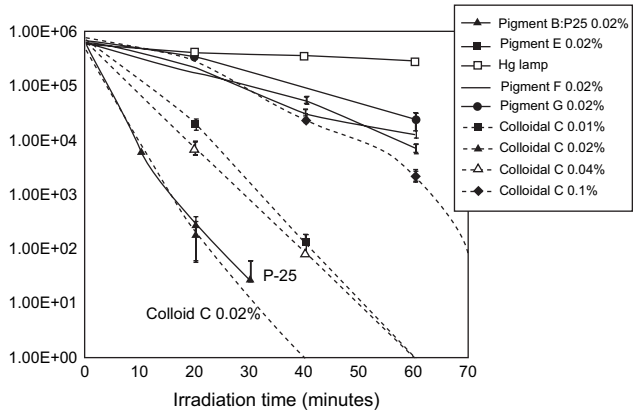

Fig. 5. Photocatalytic bactericidal effect for C colloid at different concentrations (unstirred). The effects of pigments B, D, E, F, G are displayed for comparison.

colloid dispersion C and P25 having the greatest effects. However, the experimental conditions used did provide some confounding factors which required clarification in order to identify the best experimental method and the most effect pigments in terms of antibacterial activity.

In general, the antimicrobial effect increased with increasing concentration (Fig. 3) up to 0.04%. The activity of the nanopigment E was comparable to that of the P25 pigment, followed by F and G and with little difference between A, H, D and the mercury lamp control (Fig. 4). Similar results were observed at 0.02%.

For the nanopigments E, F, G, a further enhanced effect was noted at 0.1%, but the effect of P25 was reduced.

In unstirred conditions, only pigment C, the colloid dispersion, gave results comparable with P25 (Fig. 5). Also, as with P25, activity of C increased from 0.01 to 0.02%, but decreased from 0.02 to 0.04%, and even further at 0.1%. This is because the overall effect is a balance between the increase in available surface area of the pigment, and a decrease in light transmission through the system due to increased light scattering when the pigment loading increases.

The enhanced activity of C over its derivative pigment G was lost when C was dried and ground (Fig. 6). This finding demonstrates that the drying process has a marked effect on activity, due to a decrease in surface area during aggregation, and to a decrease in dispersion stability in water.

After planetary milling in the presence of Calgon, the effect of pigment E was comparable to those of P25, which indicated that milling reduced particle size and increased activity. At lower concentrations, 0.01 and 0.001%, an induction period was observed, probably because the chance of cells and pigment coming into contact would be reduced (or that the presence of Calgon interfered with activity). An induction period was required for all pigments which had been milled: the activity of the colloid pigment C was significantly greater than that of all milled pigments (Fig. 7), because the transmission of light was considerably greater (Fig. 8). Milling may have introduced structural defects into the crystal structures that act as recombination centres for the electrons and holes [20], thus decreasing the activity compared to that of unmilled

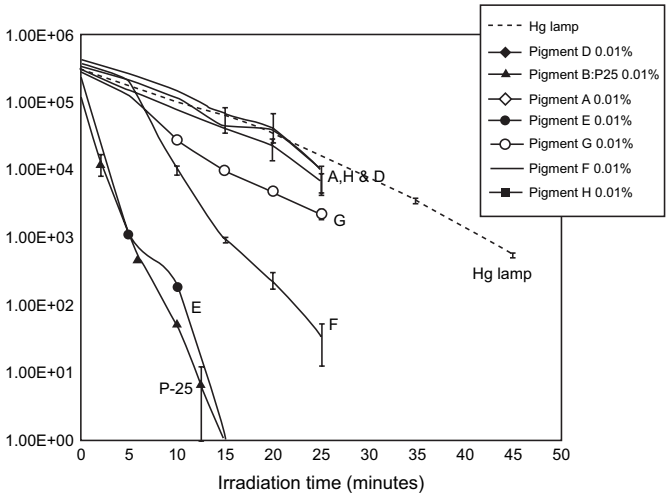

Fig. 4. Photocatalytic bactericidal effect of pigments A, B D, E, F, G, H at 0.01%, using washed cell suspensions.

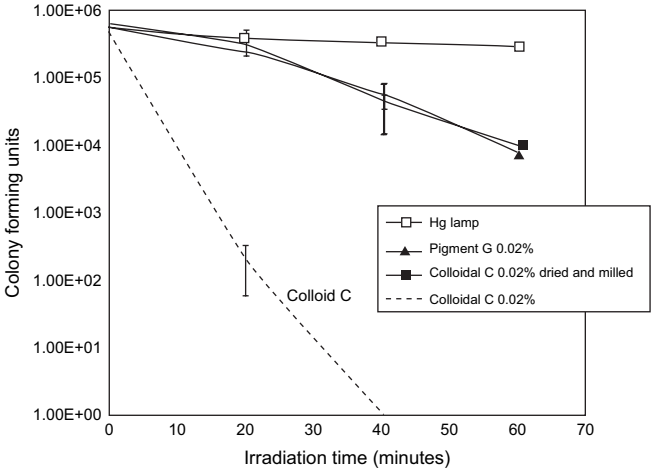

Fig. 6. Photocatalytic bactericidal effect for C colloid suspension, C dried and milled, and pigment G powder (unstirred).

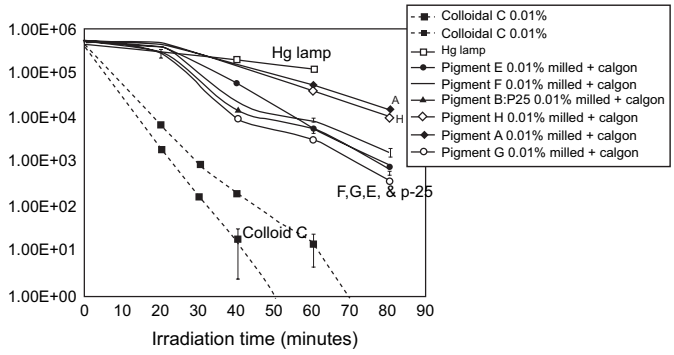

Fig. 7. Photocatalytic bactericidal effect for pigments A, B, E, F, G at 001%, milled samples dispersed in Calgon, compared with C colloid (unstirred).

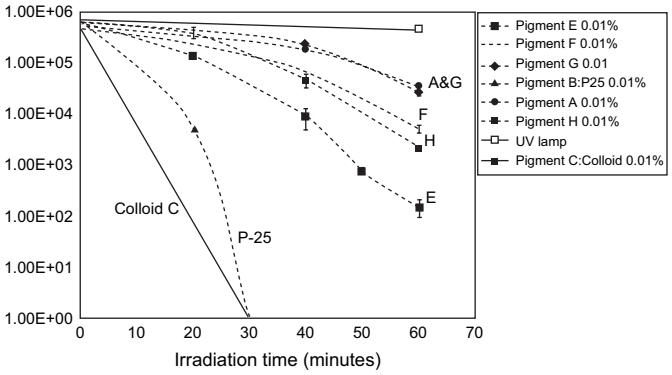

Fig. 9. Photocatalytic bactericidal effect for Calgon dispersed milled pigments A, B, E, F, G, H at 0.01%, and C colloid (stirred).

pigments. Nevertheless, the activity ranking described above, remained. In this case, the nanoparticle pigments E–G, along with P25, were the more active, with pigmentary A and nanoparticle H showing lower activity.

In stirred conditions, much clearer separation of milled pigments dispersed with Calgon was observed (Fig. 9), and the induction period was absent.

However, it was surprising that optimum activity was attained at only 0.01%. When 0.01% pigment suspensions were prepared from the powders, the same sequence of activity was noted, and activity increased at 0.1% for the powders, because since the powders contained aggregated particles, their interference with light dispersion would be less than that of the Calgon dispersed particles (Table 3).

4. Conclusions

The overall effect of activity will depend on whether more TiO_2 is activated as a consequence of increased surface area, or whether less TiO_2 is activated because less light passes through the suspension due to light scattering. Larger aggregates of particles sediment in a liquid system, and an increased concentration of pigments shows less of an antimicrobial effect since less light passes through the suspension if the cell–particle mixture is not stirred. Conversely, Calgon milled pigments which are nanometer sized also scatter light significantly at high concentrations and decrease activity (optimum loading 0.01%), thus the optimum activity is presented by nanoparticle powder aggregates. The most important aspect to consider in terms of antibacterial inactivation is the relative sizes of the titanium particles/aggregates and the bacterial cell. *E. coli* measures approximately 1×3 μm; a benzene molecule is 0.00043 μm. Porosity of the pigment has no bearing on the antimicrobial effect, whilst the chemical pollutant can diffuse into the porous pigment structure. Thus the higher surface area of pigment G did not enhance any antibacterial effect. It has been verified by disc centrifuge that the three nanoparticulate powder pigments E, F, G were aggregated into 0.7 μm particles. Thus they would all offer comparable active areas to bacteria. Only the inherent ability of the pigments to generate radicals will affect antibacterial activity. Thus the process is more sensitive to structure (crystallinity) than to texture (surface area). The antibacterial activity correlates well with the order of activity found with microwave dielectric spectroscopy, and is inversely proportional to the particle size for the nanoparticle pigments E, F and G:

$$\text{Pigment } E > F > G \ggg A$$

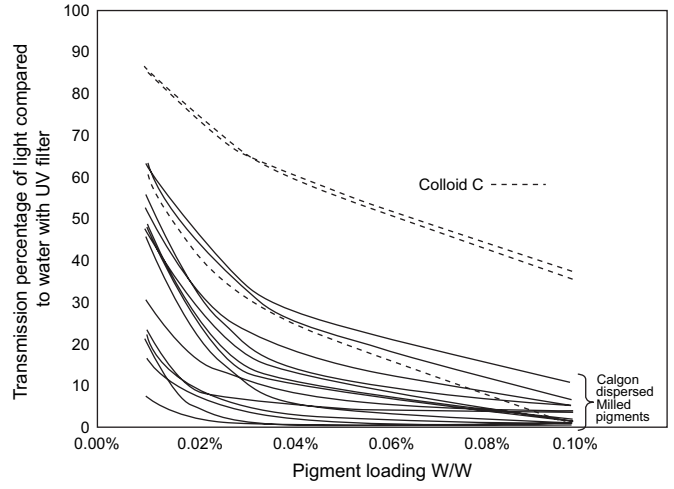

Fig. 8. Transmission of UV light at 254, 310 and 365 nm for the Calgon dispersed milled pigments and C colloid as a function of pigment concentration. The percentage on the vertical axis indicates transmission in water in the absence of pigment.

Table 3
Transmission of UV light at 254, 302 and 365 nm for pigment E suspensions at different loadings prepared from powder and from Calgon milled samples as a percentage of transmission through water and a glass filter

Pigment loading (%)	Pigment E powder (%transmission)			Pigment E milled particles in Calgon (%transmission)		
	254 nm	302 nm	365 nm	245 nm	302 nm	365 nm
0.01	83	78	81	48	17	47
0.02	69	58	65	29	8	27
0.04	45	33	42	14	3.43	10
0.1	18	7.8	11	4	0.54	0.10

Pigment E has the most reactive surface because it has fewer defects, which increase the efficiency of the photogenerated radicals [7–9]. Thus pigments calcined at higher temperatures (E > F > G) have better crystallinity and therefore higher antibacterial activities. Thus the microwave dielectric spectroscopy provides a rapid indicator of the intrinsic activity of the pigments, at least in terms of prediction of antibacterial effect. The decomposition of organic compounds such as 2-chlorophenol was proven to be more sensitive to texture (aggregate/surface area) than the inactivation of bacteria [7].

In terms of experimental variables which may affect interpretation of results, it is important to ensure that the initial concentration of bacterial inoculum is constant, and that the cells in repeat experiments are in a similar physiological state. The use of washed cell suspensions, where nutrients from the culture medium are removed prior to exposure to TiO_2, ensures that the microorganisms cannot multiply. The use of cells in culture medium potentially reduces the antimicrobial affect. This is because the organic and inorganic components of the culture medium may interfere with the activity of the pigments [10]. However, the use of culture medium as suspending fluid prevented the cells from loss of viability due to the stressful conditions provided by deionised water, thus improved the reproducibility and rigor of the method [17–19].

It is essential to ensure that exposure of cells and particles to UV light is constant and consistent across the sample vessel. Stirring of the cell–particle mixture greatly improves the antibacterial effect, keeps the pigments in suspension, and avoids light scattering by sedimented and/or static aggregates of pigment (or microorganisms). It also increases contact frequency between particles and cells.

The antibacterial activity of the nanoparticle pigments was inversely proportional to particle size, and relates to their intrinsic ability to generate active carriers for the microwave analysis. Pigments calcined at higher temperatures, consequently with fewer structural defects, are more active, because defects act as recombination centres for the electrons and holes. Hence the antibacterial efficiency of TiO_2 is not determined by surface area but by the ability to generate active carriers resulting eventually in the formation of effective chemical species such as peroxides (hydrogen peroxide) [3,4,9]. This is not surprising because of the size of bacteria relative to the pigments: the majority of the surface area offered by the pigment is sterically unavailable to the bacterial cells.

A practical advantage for the nanoparticle aggregates is arguably their improved sedimentation, which would be helpful in the final separation of cleaned water from the pigment in suspension [3,4,14–16]. The incorporation of the particles into films in order to maximise an antibacterial effect will require careful evaluation.

References

[1] Blake DM, Maness P-C, Huang Z, Wolfrum EJ, Huang J, Jacoby WA. Application of the photocatalytic chemistry of titanium dioxide to disinfection and the killing of cancer cells. Separation and Purification Methods 1999;28:1–50.

[2] Block SS, Peng VP, Goswami DW. Chemically enhanced sunlight for killing bacteria. Transactions of the American Society for Mechanical Engineers 1997;119:185–91.

[3] Kikuchi Y, Sunada K, Iyoda T, Hashimoto K, Fujishima A. Photocatalytic bactericidal effect of TiO_2 thin films: dynamic view of the active oxygen species responsible for the effect. Journal of Photochemistry and Photobiology A: Chemistry 1997;106:51–6.

[4] Sunada K, Kikuchi Y, Hashimoto K, Fujishima A. Bactericidal and detoxification effects of TiO_2 thin film photocatalysts. Environmental Science and Technology 1998;32:726–8.

[5] Linkous CA, Carter GJ, Locuson DB, Ouellette AJ, Slattery DK, Smith LA. Photocatalytic inhibition of algae growth using TiO_2, WO3 and cocatalyst modifications. Environmental Science and Technology 2000;34:4754–8.

[6] Kashige N, Kakita Y, Nakashima Y, Miake F, Watanabe K. Mechanism of the photocatalytic inactivation of *Lactobacillus casei* phage PL-1 by titania thin film. Current Microbiology 2001;42:184–9.

[7] Allen NS, Edge M, Sandoval G, Ortega A, Liauw CM, Stratton J, et al. Interrelationship of spectroscopic properties with the thermal and photochemical behaviour of titanium dioxide pigments in metallocene polyethylene and alkyd based paint films: micron versus nanoparticles. Polymer Degradation and Stability 2002;76:305–19.

[8] Corrales T, Peinado C, Allen NS, Edge M, Sandoval G, Catalina F. A chemiluminescence study of micron and nanoparticle titanium dioxide: effect on the thermal stability of metallocene polyethylene. Journal of Photochemistry and Photobiology A: Chemistry 2003;156:151–60.

[9] Allen NS, Edge M, Ortega A, Sandoval G, Liauw CM, Verran J, et al. Degradation and stabilisation of polymers and coatings: nano versus pigmentary titania particles. Polymer Degradation and Stability 2004;85:927–46.

[10] Allen NS, Edge M, Sandoval G, Verran J, Stratton J, Maltby J. Photocatalytic coatings for environmental applications. Photochemistry and Photobiology 2005;81:279–90.

[11] Verran J, Bayley K, Sandoval G, Whitehead KA. Modifying surfaces to reduce microbial retention and colonisation. In: McBain A, Allison D, Brading M, Rickard A, Verran J, Walker K, editors. Biofilm communities: order from chaos? Bioline Cardiff; 2003. p. 213–26.

[12] Edge M, Janes R, Robinson J, Allen NS, Thompson F, Warman J. Microwave photodielectric and photoconductivity studies on titanium dioxide exposed to continuous, polychromatic irradiation: part I: a novel analytical tool to assess the photoactivity of titanium dioxide. Journal of Photochemistry and Photobiology, Part A: Chemistry Education 1998;113:171–80.

[13] Janes R, Edge M, Robinson J, Rigby J, Allen NS. Microwave photodielectric and photoconductivity studies on titanium dioxide exposed to continuous polychromatic irradiation; part II: correlation of the microwave response with changes in sample microstructure during milling. Journal of Photochemistry and Photobiology, Part A: Chemistry Education 1999;127:111–5.

[14] Blake DM. Bibliography of work on the photocatalytic removal of hazardous compounds from water and air. NREL/TP-430-6084. Golden, CO: NREL; 1994.

[15] Blake DM. Bibliography of work on the photocatalytic removal of hazardous compounds from water and air. Update No 1 to June 1995. NREL/TP-473-20300. Golden, CO: NREL; 1995.

[16] Blake DM. Bibliography of work on the photocatalytic removal of hazardous compounds from water and air. Update No 2 to October 1996. NREL/TP-430-22197. Golden, CO: NREL; 1997.

[17] Verran J, Taylor RL, Lees GC. Bacterial adhesion to inert thermoplastic surfaces. Journal of Materials Science: Materials in Medicine 1996;7:597–601.

[18] Beadle IR, Verran J. The survival and growth of an environmental *Klebsiella* isolate in detergent solutions. Journal of Applied Microbiology 1999;87:764–9.

[19] Madigan MT, Martinko JM. Brock biology of microorganisms. 11th ed. New Jersey: Pearson Prentice Hall; 2006.

[20] Janes R, Edge M, Rigby J, Mourelatou D, Allen NS. The effect of sample treatment and composition on the photoluminescence of anatase pigments. Dyes and Pigments 2001;48:29–34.